International Conference on Space Optics—ICSO 2014

La Caleta, Tenerife, Canary Islands

7–10 October 2014

Edited by Zoran Sodnik, Bruno Cugny, and Nikos Karafolas

Performance verification and environmental testing of a unimorph deformable mirror for space applications

Peter Rausch

Sven Verpoort

Ulrich Wittrock

esa icso proceedings cnes

International Conference on Space Optics — ICSO 2014, edited by Zoran Sodnik, Nikos Karafolas, Bruno Cugny, Proc. of SPIE Vol. 10563, 105632Y · © 2014 ESA and CNES
CCC code: 0277-786X/17/$18 · doi: 10.1117/12.2304178

PERFORMANCE VERIFICATION AND ENVIRONMENTAL TESTING OF A UNIMORPH DEFORMABLE MIRROR FOR SPACE APPLICATIONS

Peter Rausch, Sven Verpoort, and Ulrich Wittrock
Photonics Laboratory, Münster University of Applied Sciences
Stegerwaldstraße 39, 48565 Steinfurt, Germany.
rausch@fh-muenster.de, verpoort@fh-muenster.de, wittrock@fh-muenster.de

I INTRODUCTION

Concepts for future large space telescopes require an active optics system to mitigate aberrations caused by thermal deformation and gravitational release. Such a system would allow on-site correction of wave-front errors and ease the requirements for thermal and gravitational stability of the optical train. In the course of the ESA project "Development of Adaptive Deformable Mirrors for Space Instruments" we have developed a unimorph deformable mirror designed to correct for low-order aberrations and dedicated to be used in space environment. We briefly report on design and manufacturing of the deformable mirror and present results from performance verifications and environmental testing.

II MIRROR DESIGN AND MANUFACTURING

Fig. 1 shows a cross-sectional view of the main mirror component. It is made of a piezo disc (PIC 151 from PI Ceramic) with a diameter of 84 mm and a thickness of 700 µm. The piezo disc is sandwiched between two metallic electrodes. On one side, a plain electrode serves as a common ground electrode. The electrode on the other side is structured with a ps-laser system into a 44-electrode keystone pattern, which has been optimized numerically to reproduce low order Zernike modes up to the 12th mode with large stroke and high surface fidelity [1]. Throughout this proceeding we use the Zernike notation of Wyant and Creath [2]. Three arms are cut out of the disc with the same ps-laser system used to structure the back side electrode. We use the ps-laser system to avoid any heat affected zone, which could cause localized depolarization of the piezo material. The piezo disc is adhesively bonded to mechanical support points at the end of each arm; the monolithic arms enable an integrated, monolithic tip/tilt functionality.

Our fabrication process allows the use of prefabricated superpolished and dielectrically coated glass substrates. This guarantees highly reflective (R > 99.998 %) and extremely low scattering optical surfaces, which rival the best available passive optics. The glass substrate is a 550 µm thick disc made of N-BK10 with a diameter of 64 mm. It is adhesively bonded to the unstructured front side of the piezo disc with a low-outgassing, space qualified two-component epoxy (Epo-Tek 353ND). With that same adhesive, steel segments made of the Fe-Ni-alloy Kovar are adhesively bonded to the arms of the piezo disc to facilitate tip/tilt actuation.

If a voltage is applied to the electrodes, the piezoelectric disc deforms due to the inverse piezoelectric effect. The in-plane and out-of-plane deformation is proportional to the piezoelectric coefficients d_{31} and d_{33}, respectively. While the out-of-plane deformation of the piezo disc results in a dimple of only tens of nanometers height, the in-plane deformation induces stress between the active piezo disc and the passive glass substrate (or the passive steel segments), which causes the laminate to deform locally with an amplitude of several µm.

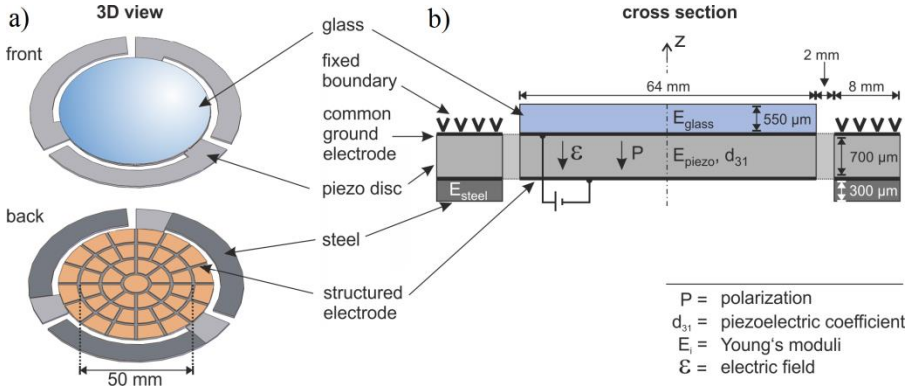

Fig. 1 a) Three-dimensional view of the deformable mirror
b) Cross-sectional view

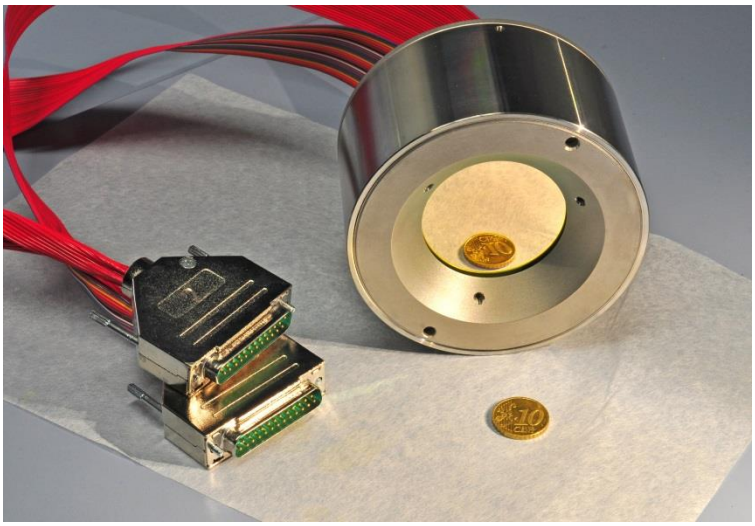

Fig. 2 Photograph of the deformable mirror DM-1

A key feature of our deformable mirror is the remarkably simple design, which allows for a flexible choice of the used materials. To mitigate the influence of temperature changes on the mirror, we chose materials that match the coefficient of thermal expansion (CTE) of the piezo material. Experiments have shown that the CTE of N-BK10 and the Fe-Ni alloy Kovar represent the best match to the CTE of PIC 151 over a wide temperature range [3]. Like the steel segments bonded onto the arms of the piezo disc, all other mechanical support parts are made of Kovar.

After bonding the three-arm structure consisting of the piezo disc with glass substrate and steel segments to a three-point mounting ring, the thereby obtained unit is attached to the mirror housing. A detailed description of design and manufacture will be given in [4]. To date, we have manufactured four deformable mirrors, DM-1 to DM-4. A photograph of the deformable mirror DM-1 is shown in Fig. 2.

III Performance Verification

A. Mirror Flattening

The prefabricated piezo discs have a poor surface quality of mainly astigmatic shape. Conventional grinding and lapping mitigates the initial deformation to a certain degree. Moreover, due to the large stroke of the mirror and the low order of the initial deformation, the mirror is able to fully compensate for its unpowered deformation without impairing its dynamic range significantly. The actively flattened surfaces of DM-1 to DM-3 are shown in Fig. 3. Despite the low amplitude print-through effect caused by the electrode pattern, the current mirror generation enables surface fidelities exceeding Strehl ratios of 0.95. This was made possible by continually improving the bonding processes, which are currently further refined. Note that the surface of DM-1 was measured with a Shack-Hartman wave-front sensor (SHS), which could not resolve the fine structures of the print-through properly.

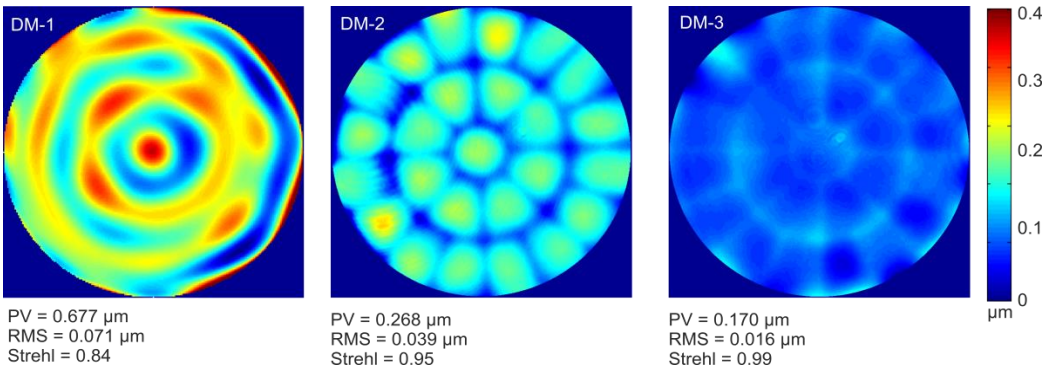

Fig. 3 Actively flattened mirror surfaces of DM-1,-2 and -3. DM-1 was measured with a Shack-Hartmann wave-front sensor, DM-2 and DM-3 were measured interferometrically

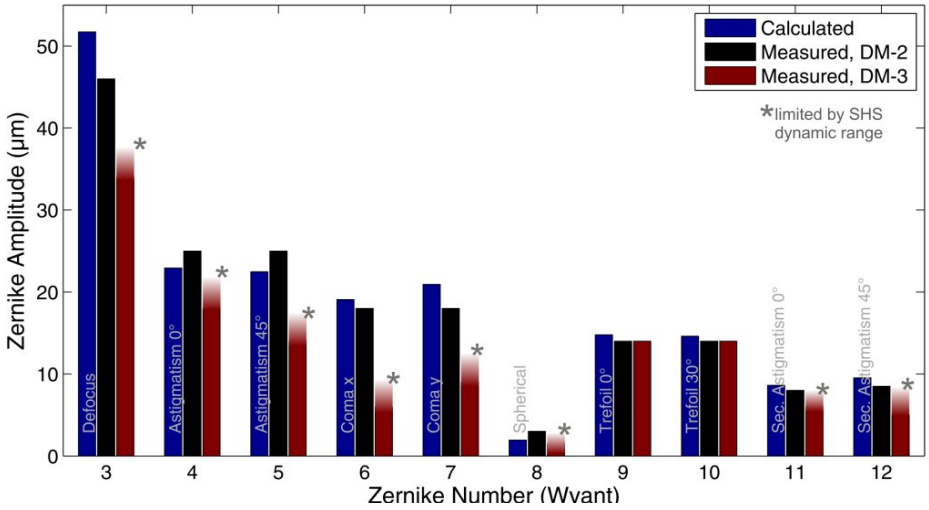

Fig. 4 Measured Zernike amplitudes along with the calculated Zernike amplitudes for DM-2 and DM-3

B. Zernike Amplitudes and Fidelities

The surface figures of the Zernike modes Z_1 to Z_{12} have been applied to the deformable mirrors in closed-loop operation to determine the maximum possible amplitudes. The loop operation started at amplitudes of 0.5 µm for every Zernike mode. The amplitude was raised in steps of 0.5 µm until one of the following criteria arose:

- The residual RMS surface deformation from the target surface exceeded λ/14 @ λ = 1064 nm (Maréchal-criterion)
- The required voltage exceeded the maximum allowed voltage of +/-400 V
- The surface deformation exceeds the dynamic range of the utilized wave-front sensor

The comparison of measured and numerically calculated maximum Zernike amplitudes is shown in Fig. 4 for DM-2 and DM-3. The measured amplitudes correspond well with the numerically calculated Zernike amplitudes, the stroke even exceeds the requirements from the statement of work. In defocus mode (Z_3), a stroke of 45 µm was achieved (30 µm required), the trefoil modes ($Z_{9,10}$) were reproduced with a stroke of 15 µm (5 µm required).

Note that the discrepancy between calculated and measured maximum amplitudes of DM-3 originates from exceeding the dynamic range of the utilized Shack-Hartmann wave-front sensor for certain Zernike modes and is not a miscalculation. Fig. 5 shows interferograms of certain low order Zernike modes at high stroke.

B. Control Bandwidth

The mirror was driven in open loop operation at varying loop frequencies. The results for loop bandwidths ranging from 1 Hz to a maximum of 123 Hz are shown in Fig 6. As can be seen, the maximum achieved amplitudes of the respective Zernike modes exhibit a significant drop between 57 Hz and 100 Hz. This can be understood in terms of the mirror´s response to a step-like voltage signal. The response is influenced by piezoelectric creep, and by the limited power that the high voltage driver can deliver. This results in a finite electrical loading time of each actuator. Typical settling times range between 10 ms and 100 ms, the exact value depending on the input voltage. The combination of creep and actuator loading allows sensibly driving the mirror with frequencies up to approximately 50 Hz.

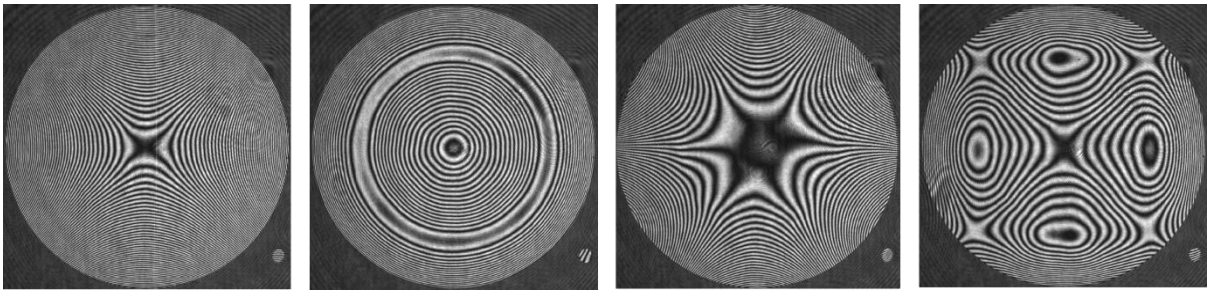

Fig. 5 Interferograms of certain low-order Zernike modes (from left to right: Z_4, Z_8, Z_{10}, Z_{11}), reproduced with high stroke

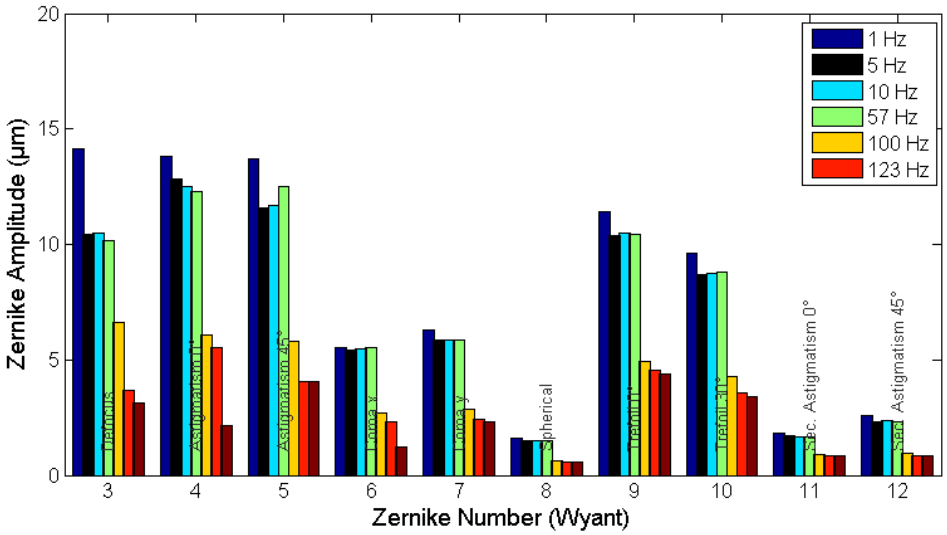

Fig. 6 Zernike amplitudes in open-loop operation at varying control loop bandwidths

IV Environmental Testing

To verify the compatibility with space environment, the mirror must be subjected to thermal vacuum, ionizing irradiation, and vibration tests. The conducted environmental tests along with the results will be presented in the following.

A. Performance in thermal vacuum

The deformable mirror DM-1 was subjected to thermal cycling in a vacuum chamber at EADS Astrium. Measurements of the mirror surface at different temperatures between 100 K and 300 K were conducted with a high resolution Shack-Hartmann wave-front sensor (116 x 116 lenslets), located in front of the vacuum chamber. A schematic view along with a photograph of the experimental setup is shown in Fig. 7. Performance measurements were conducted at thermal equilibrium. The surface figures of the Zernike modes Z_1 to Z_{10} have been applied to the deformable mirrors in closed-loop operation to determine the maximum possible amplitudes in the same fashion as described in the previous section.

Fig. 8 shows the maximum Zernike amplitudes at varying ambient temperatures, as well as after 8 temperature cycles between 100 K and 300 K. The drop in amplitude at lower temperatures is due to the decrease of the piezoelectric coefficient, which decreases with approximately 0.4% per Kelvin [5]. The achieved Zernike amplitudes after cycling are similar to those before cycling, no degradation could be observed. Note that due to an issue with the high-voltage driver electronics, the performance measurements shown in Fig. 8 were conducted with only half the maximum allowed voltage the mirror could be driven with. We have also conducted performance measurements after thermal cycling between -10°C and 40°C, with no degradation observed either.

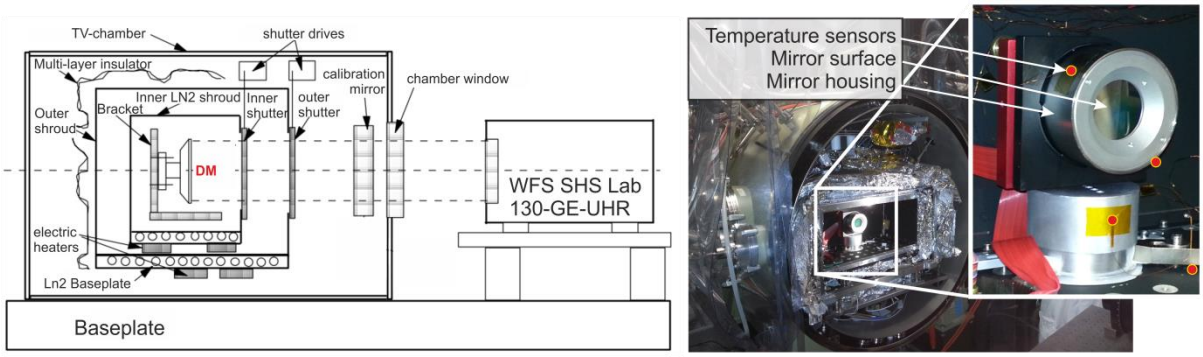

Fig. 7 Left: Schematic of the thermal vacuum performance verification test setup. Right: Deformable mirror in the open chamber. The red dots indicate the positions of temperature sensors in proximity of the mirror.

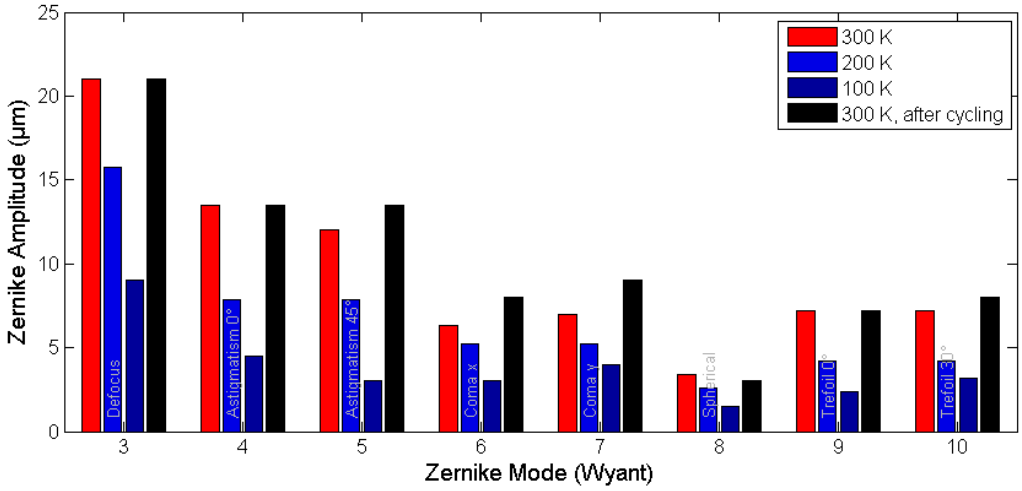

Fig. 8 Maximum achieved relative Zernike amplitudes of DM-1 in thermal vacuum at different temperatures, and after completion of 8 thermal cycles between 100 K and 300 K

B. Vibration tests

The deformable mirror DM-1 was submitted to sinusoidal and random vibration tests at EADS Astrium. The designated test levels are given in table 1, the test setup is shown in Fig. 9. Each test step was preceded and followed by a low-level 0.5 g sweep to determine the system´s resonance frequencies.
Fig. 9 shows the deformable mirror DM-1 attached to the adapter cube of the shaker system. Two accelerometers (control sensors 1 and 2) act as feedback sensors for the shaker system, another two accelerometers (vibration sensor 1 and 2) record the response of the deformable mirror. The vibration sensors were attached to the mirror housing, rather than to the piezo disc, which is the most delicate part of the DM. The mechanical parts made of the steel-alloy Kovar mainly contribute to the final mirror weight of 1.8 kg. The deformable component, consisting of the piezo disc with steel segments and glass substrate weighs 35 g, which is less than 2 % of the total mass. Hence, the contribution from the light, delicate parts may be hard to detect by the acceleration sensors which were attached to the much heavier mirror housing. It is therefore conceivable that the response recorded by the vibration sensors is mainly governed by the response of the mechanical mirror parts rather than by the response of the piezo disc.

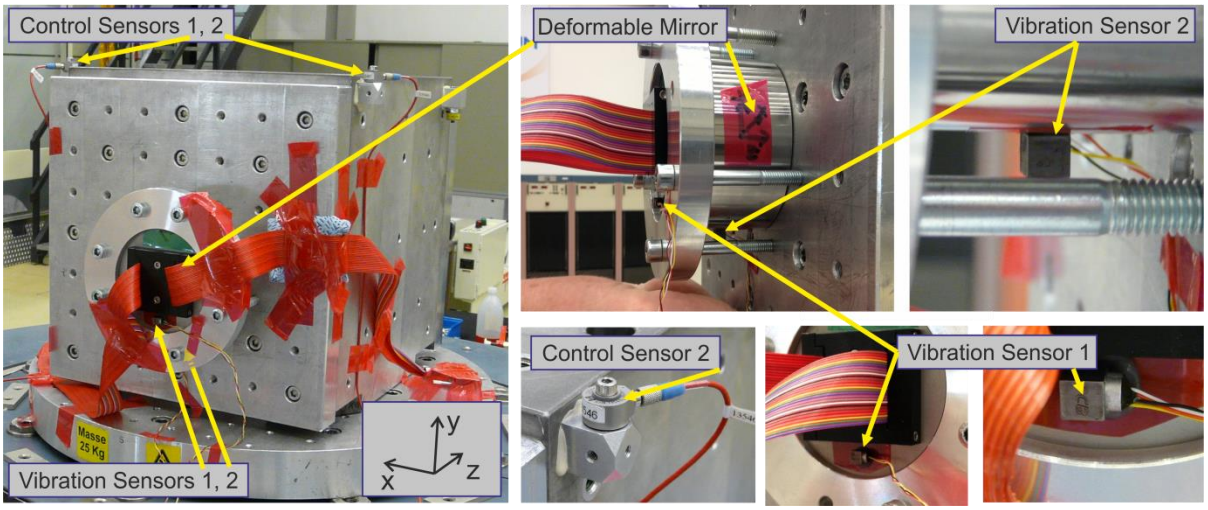

Fig. 9 Vibration test setup and positioning of the vibration and control accelerometers

Table 1 – Vibration Test Levels

Type	Frequency	Sweep rate/ Slope	Test Levels	Remarks
Sinusoidal vibration	(5-21) Hz (21-60) Hz (60-100) Hz	2 Oct/min	11 mm (0 – peak) 20 g (0 – peak) 6 g (0 – peak)	No notching allowed over full frequency range
Random vibration OOP direction	(20-100) Hz (100-400) Hz (400-2000) Hz	3.0 dB/Oct 0.0 dB/Oct -3.0 dB/Oct	(0.06 – 0.35) g^2/Hz 0.35 g^2/Hz (0.35 – 0.01) g^2/Hz	2 minutes per axis, 18.6 g rms
Random vibration IP direction	(20-100) Hz (100-400) Hz (400-2000) Hz	3.0 dB/Oct 0.0 dB/Oct -3.0 dB/Oct	0.06 – 0.2) g^2/Hz 0.2 g^2/Hz (0.2 – 0.01) g^2/Hz	2 minutes per axis, 14.1 g rms

Fig. 10 shows the transfer functions from the three low-level sweeps recorded by the acceleration sensor 2, attached to the mirror housing in proximity of the piezo disc. One sweep was conducted prior to testing, one was conducted after the sine vibration test, and the last one after the random vibration test in out-of-plane (OOP) direction. As can be seen, the response shows a deviation around 1820 Hz after the random vibration test compared to the other two sweeps. This may indicate a corruption which occurred during the random vibration test.

After the low-level sweep following the random vibration test in OOP direction, the DM was detached from the shaker and visually inspected. The upper part of Fig. 11 shows an image of the front side of the DM directly after the vibration test. One can see fine debris clinging to the adhesive side of the Kapton protection tape. Disassemblement of the DM revealed that the piezo spiral arms broke off the central disc. FEM simulations yielded that the sites of fracture coincide with regions where the piezo disc exhibits the most stress when elongated. The results of the simulation along with the sites of fracture are shown in the lower part of Fig 11.

To improve the resilience of the three-arm structure towards vibrations, we have designed two types of three-arm structure, referred to as the “spiral arm design” and the “bridge design”. The two designs are depicted in Fig. 12. In the bridge design, further mechanical stability is achieved by connecting the end of each spiral arm to the crosspiece of the neighbouring arm, thus creating a bridge-like structure.

Numerical calculations yielded a reduction of the van-Mises stress by a factor of 4 in the bridge design when applying load in arbitrary directions, the tip/tilt deformation is reduced by a factor 4 as well. The out-of-plane elongation under load is reduced by a full order of magnitude. The first two mirrors feature the spiral arm design, DM-3 and DM-4 were made in the bridge design. Vibration tests of the mirrors with bridge design are imminent.

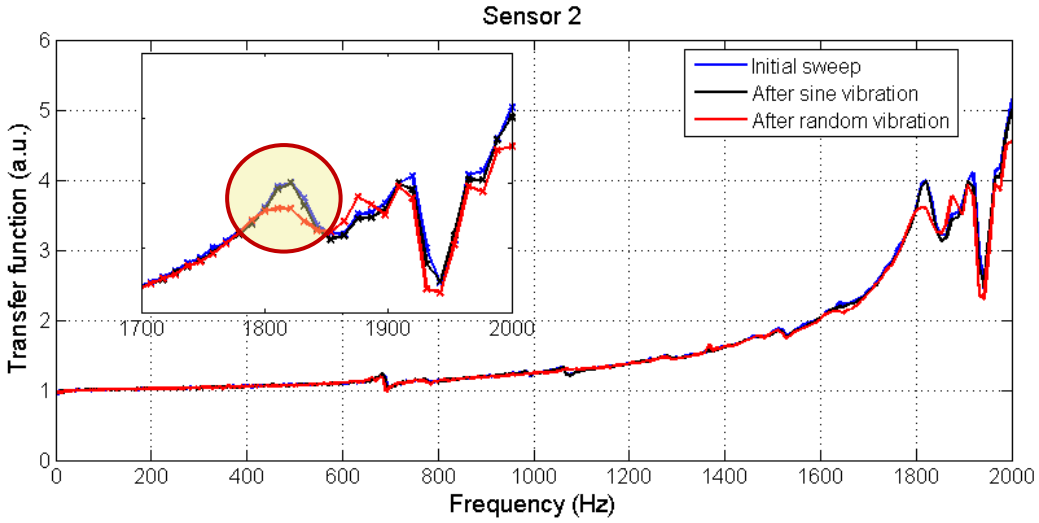

Fig. 10 Transfer functions recorded by sensor 2 for the three low-g sweeps

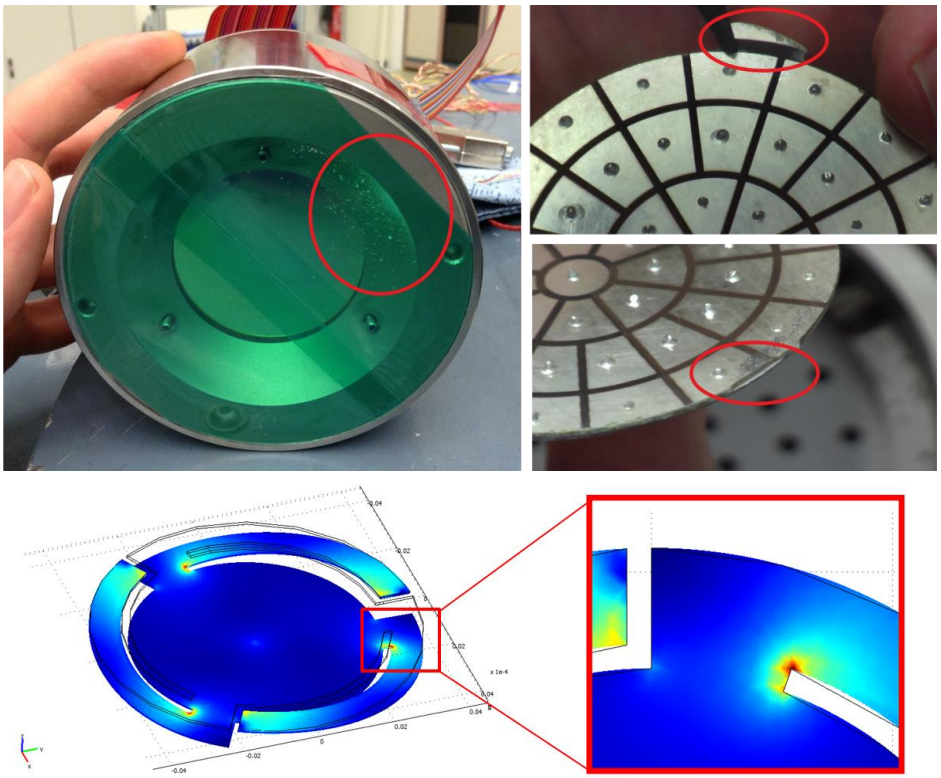

Fig. 11 **Top**: Debris stuck on the Kapton protection foil directly after the vibration test along with an image of the broken spiral arm structure
Bottom: Numerically calculated van-Mises stress inside the piezo disc when elongated

C. Irradiation tests

The deformable mirror DM-2 was subjected to gamma irradiation at ESTEC´s Co60-facility. A total dose of 50 krad (Si) at a dose rate of 1 krad/h was applied at atmospheric pressure and room temperature.

Prior and after irradiation, the mirrors performance was tested by applying a voltage of 100 V to every actuator and measuring the response. No degradation of the actuator response was observed.

Proton irradiation tests are imminent.

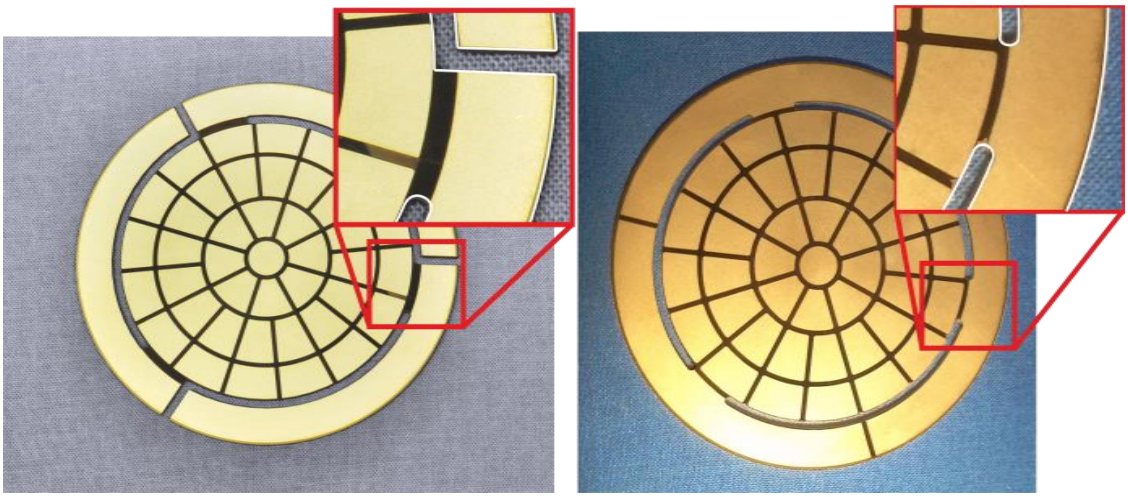

Fig. 12 Spiral arm design (left), and bridge design (right)

V Conclusions

We have presented results from performance verifications and environmental tests of a unimorph deformable mirror. The performance of the mirror regarding stroke and surface fidelity is very good, exceeding the demanded requirements. The conducted environmental tests revealed that the mirror is space compatible regarding ionizing irradiation and vast temperature changes. The athermal design allows operating the mirror at temperatures as low as 100 K. The initial piezo design (spiral arm design) is not able to withstand random vibrations. Testing of the more robust redesign (bridge design) is imminent.

VI Acknowledgement

The authors gratefully acknowledge support for the work presented by the European Space Agency under contract number 4000104030/10/NL/EM.

REFERENCES

[1] S. Verpoort and U. Wittrock, "Actuator patterns for unimorph and bimorph deformable mirrors," in *Applied Optics*, Vol. 49, No. 31, G37-G46, 2010

[2] J.C. Wyant, K. Creath, "Basic Wavefront Aberration Theory for Optical Metrology," in *Applied Optics and Optical Engineering*, vol. XI, pp. 1-51, 1982.

[3] S. Verpoort, P. Rausch, and U. Wittrock, "Novel Unimorph Deformable Mirror for Space Applications," *in Proceedings of the 9th International Conference on Space Optics (ICSO)*, Ajaccio, Corse (2012).

[4] P. Rausch, S. Verpoort, and U. Wittrock, "Design, Manufacturing, and Characterization of a Unimorph Deformable Mirror for Space Applications", unpublished

[5] http://www.piezosystem.com/fileadmin/redakteure/bilder/Sonstige/Piezofibel/Piezoline_engl_komplett.pdf